Generation of Bioengineered Corneas with Decellularized Xenografts and Human Keratocytes

Miguel Gonzalez-Andrades,[1,2] *Juan de la Cruz Cardona,*[3] *Ana Maria Ionescu,*[3] *Antonio Campos,*[1] *Maria del Mar Perez,*[3] *and Miguel Alaminos*[1]

Purpose. Decellularization of animal corneas is a promising method for the development of artificial human corneas by tissue engineering. In this study, two different decellularization protocols were evaluated to determine which one is able to best preserve the histologic structure, composition, and optical behavior of decellularized porcine corneas. Then, these corneas were recellularized with human keratocytes to obtain a partial human corneal substitute.

Methods. Two different decellularization protocols were applied, using NaCl and SDS, to determine which one is able to best preserve the histologic structure, composition, and optical behavior of the decellularized corneas. Then, those decellularized corneas that showed the most appropriate results were recellularized with human keratocytes and evaluated at the histologic, biochemical, and optical levels for use in regenerative medicine.

Results. The results showed that 1.5 M NaCl treatment of porcine corneas is able to generate an acellular corneal stroma with adequate histologic and optical properties and that human keratocytes are able to penetrate and spread within this scaffold with proper levels of cell differentiation. In contrast, 0.1% SDS treatment of porcine corneas resulted in high levels of fibril disorganization and poor optical behavior of these corneas.

Conclusions. In conclusion, the authors suggest that the decellularization of animal corneas with 1.5 M NaCl represents a useful method for the development of human bioengineered corneas with therapeutic potential. (*Invest Ophthalmol Vis Sci.* 2011;52:215–222) DOI:10.1167/iovs.09-4773

The cornea is the most important element in visual function regarding the refractive power of the different elements of the eye.[1] This property is due to the organized, transparent structure of the corneal stroma, which is essential for proper visual function.[2,3] Moreover, the cornea constitutes a tight barrier that protects the internal elements of the eye from the aggression of the external environment.[4]

From the Departments of [1]Histology and [3]Optics, University of Granada, Granada, Spain; and the [2]Division of Ophthalmology, University Hospital San Cecilio, Granada, Spain.

Supported by the Plan Nacional de Investigación Científica, Desarrollo e Innovación Tecnológica (I+D+I), Instituto de Salud Carlos III (ISCIII), Subdirección General de Evaluación y Fomento de la Investigación (FIS PI08/614), and by PI0132/2007 from the Health Department of the Andalusian Regional Government, Spain.

Submitted for publication October 14, 2009; revised February 28 and June 2, 2010; accepted August 3, 2010.

Disclosure: **M. González-Andrades**, None; **J.C. Cardona**, None; **A.M. Ionescu**, None; **A. Campos**, None; **M.M. Pérez**, None; **M. Alaminos**, None

Corresponding author: Miguel Alaminos, Department of Histology, University of Granada, Avenida de Madrid 11, E-18012, Granada, Spain; malaminos@ugr.es.

There are numerous diseases that can affect this highly organized structure, leading to corneal opacification, visual impairment, and even blindness. Moreover, we must take into account that the only treatment at the moment for most of these diseases is corneal transplantation.[5] Nevertheless, there are two major disadvantages related to this procedure: graft rejection and the lack of donors. For that reason, from a clinical point of view it would be very useful to generate a corneal substitute for the human cornea.[6–8]

Nowadays, corneal tissue engineering has emerged as a promising option to solve all these problems. At the time of this writing, several functional artificial corneas based on different types of matrices such as polymers, collagen, or fibrin-agarose scaffolds have been developed.[4,8–10] Although these bioengineered corneal constructs displayed proper levels of biocompatibility, mechanical stability, optical transparency, and refractive power, a promising alternative to these artificial corneas would be the use of corneal xenografts. However, one of the main limits to xenotransplantation in humans is the existence of natural antibodies to the terminal galactose α 1,3 galactose (α-gal) epitope expressed in the cell membranes of all mammals except those of humans and old world primates; these antibodies can mediate hyperacute or delayed rejection of the xenograft.[11]

In this context, several research groups have chosen the porcine cornea as a suitable xenogeneic corneal matrix substitute to be decellularized, applying different decellularization procedures previously optimized in other tissues different from the cornea.[12] Ideally, a good cornea decellularization protocol should be able to fulfill four major gold-standard criteria: (1) proper decellularization efficiency, with elimination of all cells and cell debris from the decellularized xenograft; (2) proper elimination of all α-gal epitopes; (3) proper possibility of recellularization of the decellularized tissues using host cells; (4) proper optical behavior of the descellularized corneas. However, all methods described to date for cornea decellularization vary significantly in their efficacy, including the possibility of further recellularization of the acellular matrix.[13–17] In fact, recellularization of decellularized corneas with allogenic human keratocytes had not been achieved at the time of this writing.

In the case of the cornea, all the above-mentioned criteria are essential, since transparency of the cornea is highly dependent on two major parameters: the structure of the stromal matrix[18] and the shape, size, density, and structure of the corneal cells.[19] In fact, Meek et al.[18] considered the cornea to be a structure made only of collagen fibrils and extrafibrillar matrix, and they were able to demonstrate that fibril disordering, increased refractive index mismatch, and increased corneal thickness can account for an increase in light-scattering in human cornea using the direct summation of fields (DSF) method.[20] In contrast, Mourant et al.[19] suggest that the cells themselves would be responsible for the light scattered in small angles, the nuclei would be relevant in the greater angles,

and small organelles such as mitochondria and lysosomes, would be responsible for the light scattered in large angles. Both the extracellular matrix and the corneal cells play a key role in the spectral transmittance function of the human cornea, which seems to be dominated by light-scattering processes rather than by absorption, with the latter being relevant only in the extreme short wavelength.[21]

In the present study, we optimized and evaluated two different decellularization methods, using NaCl and SDS to determine which one is able to best preserve the histologic structure, composition, and optical behavior of the decellularized corneas. Then, those decellularized corneas that showed the most appropriate results were recellularized with human keratocytes and evaluated at the histologic, biochemical, and optical levels for use in regenerative medicine.

Material and Methods

Decellularization of Porcine Corneas

Ninety fresh porcine corneas were obtained from adult pigs immediately after their death at a local slaughterhouse. The eyes selected for the study had integral corneal surface with a horizontal corneal diameter of 12 to 14 mm. The native porcine cornea (NPC) with 2-mm scleral ring was removed with a 16-mm corneal trephine. Ten NPCs were used as controls. The corneal epithelium and endothelium were removed, using 4 mg/mL Dispase II for 45 minutes at 37°C. All the solutions in which porcine corneas were immersed had a mass ratio of 20:1 (solution:cornea). Corneas were washed thoroughly with 10% antibiotic–antimycotic solution (Invitrogen-Gibco, Carlsbad, CA) in phosphate-buffered saline (PBS) for 10 minutes and then washed in PBS. Two independent decellularization processes were performed: one using 1.5 M NaCl (applied to 50 corneas) and the other using 0.1% SDS in PBS (applied to 30 corneas). Both protocols were carried out with continuous shaking (200 rpm) for 12 hours at room temperature. Then, acellular porcine corneas (APCs) were washed three times with PBS for 30 minutes at room temperature with continuous shaking (200 rpm). Once decellularized and to eliminate the liquid excess, the APCs were kept in a specific chamber for 30 minutes. This chamber consisted of a 5-cm diameter stage where the APCs were introduced between several layers of paper towels (3MM; Whatman, Qiagen, Valencia, CA).

Obtaining Human Keratocytes

Corneal–scleral limbal rims of 14-mm diameter were obtained at the University Hospital of San Cecilio (Granada, Spain), after the removal of ±7-mm central corneal buttons for corneal transplantation. Stromal keratocytes were isolated from fragments of corneal stroma that remained attached to the sclerocorneal limbus, by using collagenase I (Invitrogen- Gibco) at 37°C for 6 hours. The culture medium used was DMEM supplemented (DMEMs) with 10% fetal calf serum, 4 mM L-glutamine, and 1% antibiotic–antimycotic solution (Invitrogen-Gibco). All cells were incubated at 37°C in 5% carbon dioxide under standard culture conditions.

All experimental protocols, including the use of both human and animal tissues, were approved by the Institutional Review Board and Institutional Animal Care and Use Committee of Granada University Hospital San Cecilio. This work adhered to the Declaration of Helsinki and the ARVO Statement for the Use of Animals in Ophthalmic and Vision Research. For the use of human corneal rims after trephination of the donor buttons for research purposes, a written approval was obtained from the legal representatives of the donors according to the protocols established by the Spanish National Organization for Human Transplantation (ONT).

Recellularization of APCs

After washing the APCs with PBS, we immersed 20 of them treated with NaCl in DMEMs (20:1 mass ratio) for 3 hours. Then, the culture medium was removed, and 200,000 human keratocytes were seeded on the corneal surface at room temperature. After 2 hours, the corneas were completely submerged in DMEMs to a mass ratio of 20:1. All recellularized corneas (RCs) were incubated at 37°C in 5% carbon dioxide under standard culture conditions for 14 days. This recellularization process was applied only to APCs decellularized with the protocol that most efficiently preserved the original structure of the native cornea (i.e., corneas decellularized with NaCl).

Histology and Fluorescence Immunohistochemistry Evaluation

For light microscopy, native and bioengineered corneas were fixed in 4% formaldehyde, dehydrated in an ethanol series, and embedded in paraffin. Cross sections were cut, 4 μm thick, stained with hematoxylin and eosin or Alcian blue, and examined with a light microscope.

The expression of α-gal epitope and aldehyde dehydrogenase 1 (ALDH1) was determined by fluorescence immunohistochemistry, using paraffin-embedded tissue sections corresponding to NPCs, APCs, and RCs.

First, paraffin was removed from the tissue sections, using xylene, and the samples were rehydrated in water through a graded series of alcohols (100%, 96%, 70%, 50%, and water). Then we used a 0.01 M citrate buffer (pH 6.0) at 95°C for 10 minutes for antigen retrieval. After blocking any unspecific binding sites using bovine serum albumin, we incubated the samples with the primary antibodies for 1 hour at room temperature. Mouse monoclonal antibodies against the α-gal epitope (ALX-801-090-L002, clone M86; Alexis Biochemicals, Lausen, Switzerland) were applied 1:20. Goat polyclonal antibody against ALDH1 (PC713, purified goat polyclonal antibody; Calbiochem, Darmstadt, Germany) was used 1:300. Incubation with secondary antibodies was carried out for 30 minutes using FITC-conjugated anti-mouse antibody (F9137, dilution 1:500; Sigma-Aldrich, St. Louis, MO) or CY3-conjugated anti-goat antibody (C-2821, dilution 1:500; Sigma-Aldrich). Finally, the slides were counterstained with DAPI and photographed by light microscope (Eclipse i90; Nikon, Tokyo, Japan).

To determine the efficiency of both the decellularization and the recellularization methods, histologic images corresponding to each tissue type were obtained. Then, the number of remaining nuclear debris (60 decellularized corneas: 30 treated with NaCl and 30 treated with SDS) and the number of keratocytes (20 recellularized corneas) were determined per each field, by using imaging software (NIS-Elements; Nikon) in the automatic detection mode, taking into account that 12 microscopic fields per sample were used for the statistical analysis. All values obtained in this work corresponded to corneal stroma fields of 2700 μm^2.

Fiber Orientation Analysis and Surface Characterization

Surface characterization and analysis of stromal fiber orientation of the samples dyed with hematoxylin and eosin was performed with SurfCharJ ImageJ plug-in for surface assessment (ImageJ software, developed by Wayne Rasband, National Institutes of Health, Bethesda, MD; available at http://rsb.info.nih.gov/ij/index.html).[22] This plug-in allows for the calculation of structure orientation based on the mean resultant vector[23] and plots the frequency of azimuthal angles for estimating the preferred orientation. To analyze the fiber orientation of the whole APC, we first obtained individual hematoxylin and eosin staining pictures of the anterior and the posterior half of the APC. Then, the analysis was carried out individually for each picture, and average values were calculated.

Evaluation of the Optical Proprieties of the Corneas

Spectral distribution of the reflectance of the decellularized and recellularized corneas was determined by using a spectroradiometer, (SpectraScan PR-704; Photo Research, Inc., Chatsworth, CA) with 4% mea-

surement accuracy. The percentage of repeatability of the measurements was much lower (the SD of repeat measurements over a 15-minute period was <0.1%). The specimens were situated in a cabinet (CAC 60; Verivide Ltd., Leicester, UK) and a source simulating the spectral relative irradiance of CIE (The International Commission on Illumination) standard illuminant D65 was used. Illuminating and viewing configurations were CIE d/0° geometry. For the measurements the specimens were situated over a black-and-white background.

The measurements were made in the center of the samples. Nonsignificant differences were found between the spectral reflectance values of each place ($P > 0.05$). Before each measurement, the sample thickness was determined with an optical microscope (CO11; Olympus, Lake Success, NY).

The scattering coefficient (S) was calculated algebraically from the spectral reflectance data of each tissue using Kubelka-Munk (K-M) equations.[24,25] This phenomenologic scattering coefficient is a pure function of the physical scattering coefficient of the medium to be studied.[26]

Using the secondary optical constants (a and b) and the scattering coefficient (S) we calculated the transmittance as $T(X) = b/[a \cdot \sinh(bSX) + b \cdot \cosh(bSX)]$.

Statistical Analysis

Statistical comparison of the average number of remaining nuclear debris between NaCl- and SDS-treated APCs and fiber orientation parameters of NPCs, APCs, and RCs was carried out by using the nonparametric Mann–Whitney U test. Absolute average values for the scattering and absorbance curves were compared by using the same statistical test, whereas the trend, as determined by the shape of the curve, was compared using the VAF (value adjustment factor) test.

All tests were performed two-tailed and a Bonferroni-adjusted $P < 0.0025$ was considered as statistically significant, since up to 20 statistical tests were performed ($0.05/20 = 0.0025$).

Results

Evaluation of APCs Decellularized with SDS- and NaCl-Based Protocols

As shown in Figure 1, the macroscopical transparency level of corneas decellularized with NaCl was similar to that of the control NPC. However, SDS-treated corneas apparently showed lower transparency than the other types of corneas.

Histologic analysis, using DAPI and hematoxylin and eosin staining of APCs subjected to NaCl or SDS decellularization protocols, revealed that both methods were able to eliminate all cells previously present in the corneas, although some nuclear debris remained in both cases (Fig. 2); however, the efficiency of both decellularization methods was different and APCs treated with SDS showed a lower level of remaining nuclear debris than APCs treated with NaCl (average, 1.6 ± 1.8 for SDS and 4.5 ± 2.0 for NaCl). Differences were statistically significant ($P < 0.001$). In addition, the stroma in the APCs treated with SDS was partially disorganized in comparison to that in the NaCl-treated APCs and NPCs. Both decellularization protocols maintained the presence and the integrity of Bowman's layer and Descemet's membrane, as determined by hematoxylin and eosin (Fig. 2).

On the other hand, fiber orientation analysis using the SurfCharJ ImageJ plug-in (Fig. 2) demonstrated that APCs subjected to the NaCl decellularization protocols showed a fiber distribution that was very similar to the control NPCs, whereas SDS-treated APCs displayed a high level of fiber disorganization. In fact, the direction of the fibers of SDS-treated APCs, as determined by DAF (direction of azimuthal facets) was significantly different from that of the control NPCs ($P = 0.001$), with polar plot images showing high fiber disorientation in the anterior part of the cornea. In contrast, DAF and polar plot images of NaCl-treated APCs were comparable to those of the control NPCs ($P > 0.05$). In the same sense, polar facet orientation (both the mean PFO and variation MFOV) and surface area (SA) showed that the organization and orientation of the fibers were more similar to those of the controls for NaCl-treated APCs than for SDS-treated APCs, with differences being statistically significant only for SDS-treated APCs ($P = 0.001$ for PFO and DAF and $P < 0.001$ for SA for the comparison of NPCs and SDS-treated APCs).

Moreover, as shown in Figure 2, Alcian blue staining showed that proteoglycans were distributed throughout the NPCs, with an increase in concentration in the most anterior part of the stroma. APCs treated with NaCl presented Alcian blue dye intensity levels that were comparable to those of NPCs, except for the most anterior corneal stroma, in which stain intensity was lower than that of the NPCs. In the third place, APC treated with SDS changed this pattern, showing lower dye intensity in all the stroma in comparison to NPCs and APCs treated with NaCl. Hence, the most anterior stroma decellularized with SDS did not display any proteoglycan expression level at all.

The immunofluorescence analysis of α-gal protein expression showed regular distribution of α-gal epitope across all the thicknesses of the stroma of the NPCs (Fig. 2). Regarding the APCs, corneas treated with both kinds of decellularization protocols did not display any significant expression of α-gal epitope.

Finally, evaluation of the optical properties of the APCs showed that the spectral distribution of the transmittance and the K-M scattering coefficient of APCs treated with NaCl and SDS were very similar to those of the control NPCs, as determined by VAF analysis (VAF > 95.49% in Table 1, Fig. 3). In fact, the K-M scattering coefficient decreased with increasing wavelength, and this decrease was more pronounced for the short and medium wavelengths. In terms of transmittance, the spectral distribution of both types of APCs approximated well that of the control NPCs, although statistically significant differences were found for all samples analyzed ($P < 0.001$, Table 1).

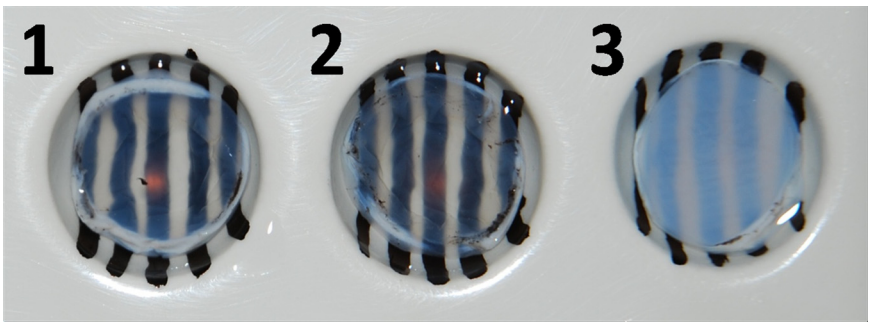

Figure 1. Macroscopical appearance of NPC (1) and corneas decellularized with 1.5M NaCl (2) and 0.1% SDS (3). All corneas were set on a black-and-white stripped background to show transparency.

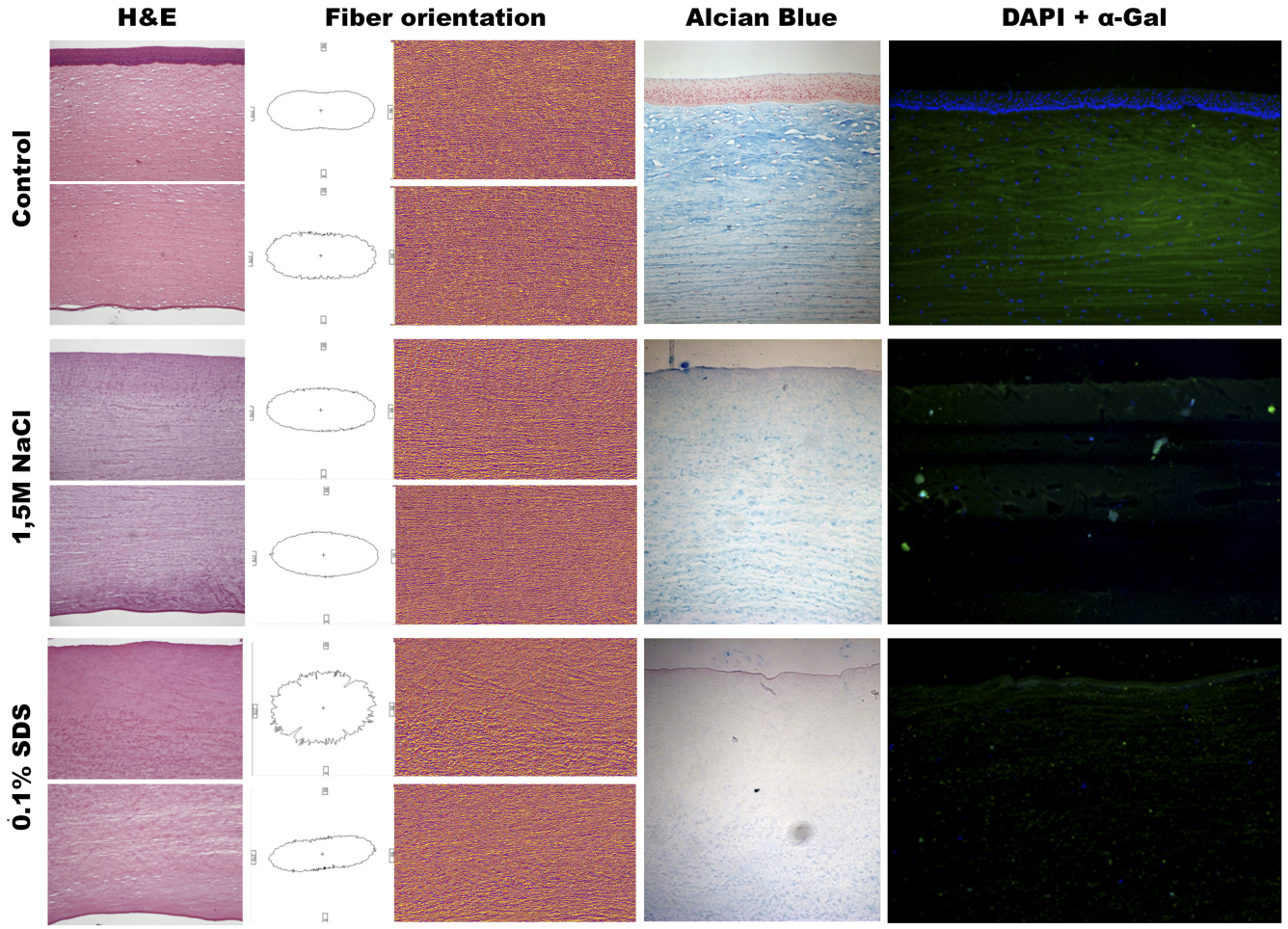

FIGURE 2. Analysis of NPC (*top row*) and corneas decellularized with 1.5 M NaCl (*middle row*) and 0.1% SDS (*bottom row*). *First column*: hematoxylin and eosin staining of the anterior and posterior regions of the corneas; *second column*: fiber orientation analysis with polar plot images; *third column*: azimuthal images; *fourth column*: Alcian blue staining of the different samples; *fifth column*: fluorescence immunohistochemistry against α-gal epitope

Recellularization Efficiency

Hematoxylin and eosin staining of APCs recellularized with human keratocytes demonstrated that human cells were able to migrate and spread into the acellular corneal stroma decellularized with NaCl (Fig. 4). These results were confirmed by DAPI fluorescence staining. Furthermore, our histologic analysis revealed that the number of cells in the recellularized APCs was comparable to that of the control NPCs (average, 11.9 ± 5.3 cells per field for recellularized APCs vs. 9.5 ± 2.1 cells per field for NPCs; $P > 0.05$), although the distribution of the cells could be more irregular in recellularized APCs in comparison with the control NPCs (Fig. 4).

Moreover, keratocytes expressed high levels of ALDH1 protein (a marker of mature keratocytes) after 3 weeks in

TABLE 1. Statistical Comparison of the Spectral Distributions of the Transmittance and the Kubelka-Munk (K-M) Scattering Coefficient of Control NPC, NaCl-Treated APC (NaCl APC), SDS-Treated APC (SDS APC) and RC

	NPC	SDS APC	NaCl APC	RC
Scattering				
NPC	—	VAF = 95.49%	VAF = 98.93%	VAF = 99.80% $P < 0.001$
SDS APC	$P < 0.001$	—	VAF = 97.98%	
NaCl APC	$P < 0.001$	$P < 0.001$	—	
Transmittance				
NPC	—	VAF = 85.39%	VAF = 94.45%	VAF = 99.48% $P < 0.001$
SDS APC	$P < 0.001$	—	VAF = 96.78%	
NaCl APC	$P < 0.001$	$P < 0.001$	—	

P-values correspond to the Mann-Whitney U statistical comparison, whereas VAF correspond to the similarity of the curves as determined by the value adjustment factor test.

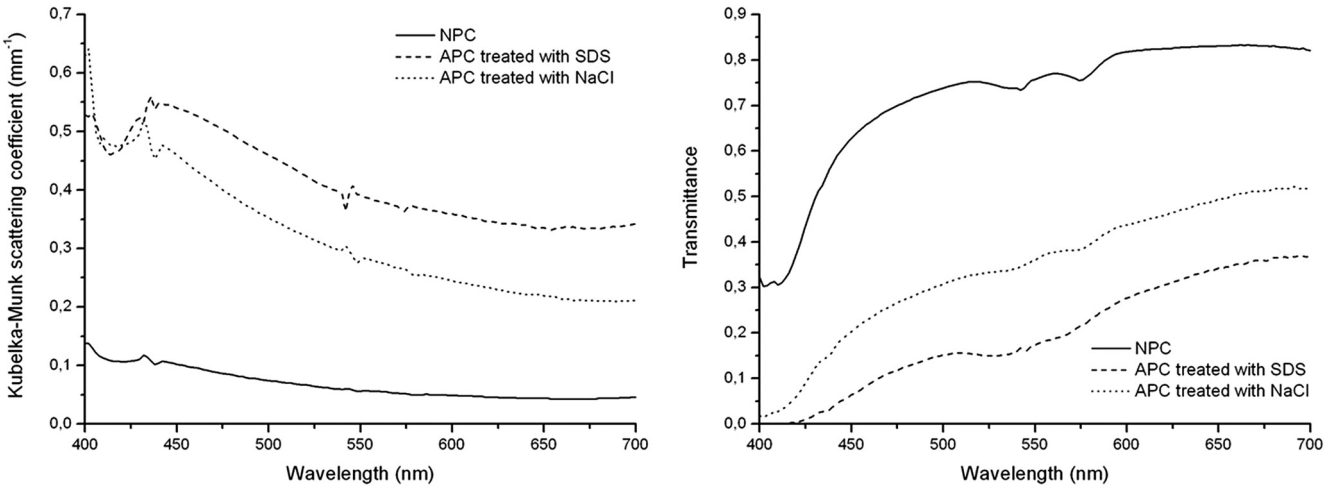

FIGURE 3. Spectral distribution of the Kubelka-Munk scattering coefficient and transmittance of the control NPCs and the APCs treated with NaCl and SDS.

culture, as demonstrated by fluorescence immunohistochemistry (Fig. 5).

On the other hand, our optical analysis revealed that the spectral behavior of the scattering coefficient and transmittance of RCs was very similar to those of the control NPCs (VAF $>$ 99.32%; Table 1). In addition, we found that the transmittance increased when corneas were recellularized, suggesting that human keratocytes may play a key role in maintaining corneal transparency. As shown in Figure 6, both the K-M scattering coefficient and the transmittance values of RCs tended to mimic those of the control corneas after 2 weeks in culture. In the same sense, both the NPCs and RCs had a spectral dependency that was proportional to the inverse of the cube of the wavelength. Statistically, we obtained significant differences for all comparisons performed ($P < 0.001$, Table 1).

DISCUSSION

Generation of artificial corneas based on decellularization methods should fulfill requirements similar to those of native human corneas, including biocompatibility, immunologic acceptance, mechanical integrity, and optical transparency.[8,13] These decellularized corneas should also provide the specific microenvironment for the stromal and epithelial cells to migrate and repopulate the tissue graft, both in vitro and in vivo.

Most of these requirements depend on the perfectly organized structure of the corneal stroma, which is very difficult to mimic in the laboratory. Moreover, human and porcine corneas have a great amount of similarities regarding their physical and chemical properties, as previously described.[14,27] In fact, porcine corneas are commonly used as an animal model due to their availability from meat-packing houses and their relative similarity to human corneas.[28] Various physical properties of porcine corneas have been investigated and compared with corneas of pigs, mice, rabbits, sheep, cats, dogs, and cows. These studies found that water, hydroxyproline and chondroitin-sulfate contents were approximately constant across the species, except for mice, and that keratin-sulfate content increased with corneal thickness, whereas dermatan-sulfate content decreased.[14] Therefore, decellularization scaffolds emerge as promising tools in tissue engineering due to their similarity to native tissues and their availability.[28]

However, one of the major problems for xenotransplantation in humans is the presence of natural human antibodies against α-gal epitope, which induces mild cellular rejection.[11]

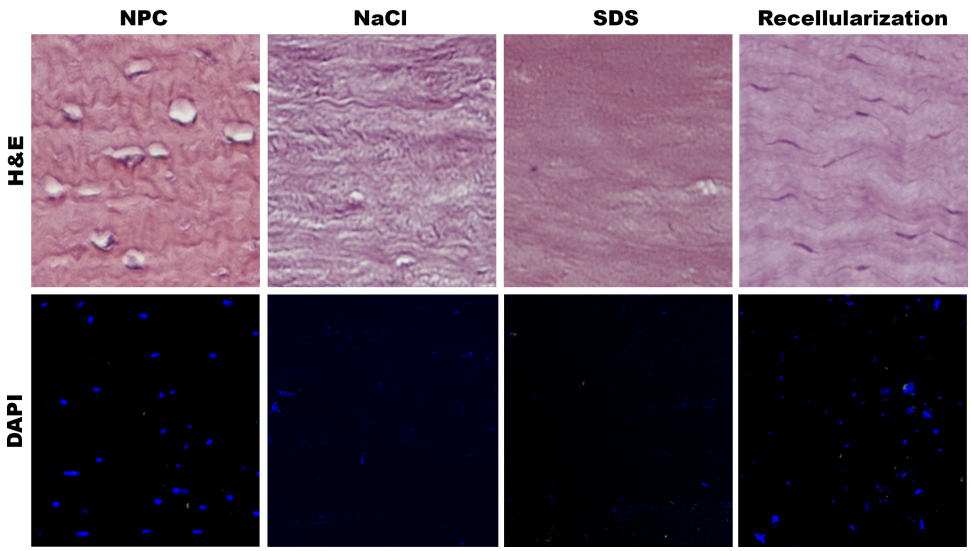

FIGURE 4. Histologic analysis of NPCs: corneas decellularized with 1.5 M NaCl and 0.1% SDS, and recellularized corneas stained with hematoxylin and eosin (*top row*) and DAPI (*bottom row*).

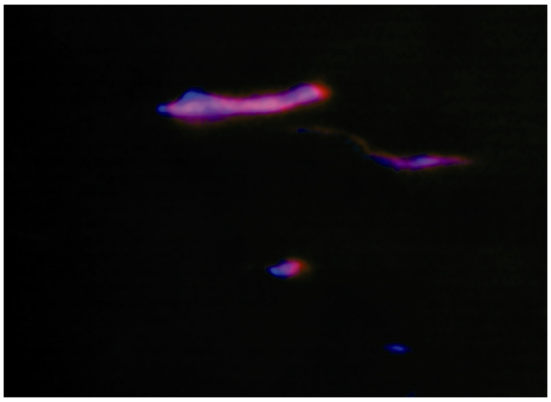

FIGURE 5. Fluorescence immunohistochemistry against ALDH1 protein showing a positive signal (*pink*) in the recellularized human keratocytes (*blue* nucleus with DAPI).

The decellularization process carried out in this study eliminated most of the α-gal epitope signal, as shown by immunofluorescence. Hence, our decellularized corneas may be immunologically accepted by a human host once implanted in vivo.

Several decellularization protocols have been described to date. However, none of them appeared to be the ideal method for application in human corneal regeneration. Some research groups have described several corneal decellularization methods using physical and chemical protocols to remove cells from the corneal xenograft.[13–17,29,30] Even when successful results have been described by these groups, there are some disadvantages involved in the majority of the protocols used.[12] In most cases, the highly organized structure of the collagen stroma fibers becomes impaired after the decellularization process, with partial elimination of some key extracellular matrix components such as proteoglycans.

In this context, NaCl and SDS have been proposed as highly efficient decellularization methods. Several research groups have previously applied NaCl along with other chemical elements to remove cells from tissues like mesangial glomerulus and dermis.[31,32] Recently, Oh et al.,[13] described the use of NaCl to decellularize anterior sliced animal stromas of 250 μm thickness. In the present study, we described two different methods based on the use of NaCl and SDS to generate a full-thickness acellular corneal stroma. Our results suggest that NaCl treatment of porcine corneas generates better results, with a fiber distribution that was very similar to that of the control NPCs, as demonstrated by histologic and surface orientation analysis. Although the protocol based on SDS treatment resulted in proper decellularization levels, the disorganization of the collagen fibers and the excessive degree of proteoglycan removal hampers the use of this type of protocol. In contrast, the use of NaCl on full-thickness corneas was able to efficiently decellularize these organs without affecting the fibril orientation or the proteoglycan composition of the decellularized cornea.

Moreover, optical analysis confirmed that the use of NaCl did not significantly disrupt the fibril orientation compared with SDS treatment, since optical scattering of NaCl-treated corneas was lower than that of SDS-treated corneas. In concordance with that, the highest transmittance levels were found for corneas treated with protocols based on NaCl, although these levels were lower than those of the NPC due to the higher scattering that was found in decellularized corneas. This high scattering may be associated with a partial disorganization of the extracellular matrix fibrils, the loss of cells within the stroma, and the change of the refractive index, because the areas that were previously populated by stromal keratocytes are now occupied by a fluid in the decellularized corneas. These factors strongly influence the increase in scattering.[18]

There are several hypotheses that have been advanced relating cornea structure and transparency. Features of the ultrastructure of the cornea, such as fibril length, most probable orientation of the fibrils, and angle between optic and geometric axis of the fibrils, can be described applying a nonrandom assembly of anisotropic fibril model to the light-scattering patterns of human cornea.[33] McCally and Farrell[34] investigated the wavelength dependency of scattering within the cornea and concluded that the range of the ordering of the collagen fibrils (e.g., short-distance versus long-distance order) would affect scattering. Therefore, estimation of the scattered light is essential to evaluate the orientation of the corneal fibrils, as with the corneal transparency. In our study, just like the results obtained by McCally and Farrell,[34] we found that the recellularized corneas treated with NaCl also adjusted to the spectral dependency of the scattering, proportional to the inverse of the cube of wavelength. This cubic wavelength dependency of the scattering in our corneas is in contrast with the Rayleigh four-power dependency, which assumes no regularity of the

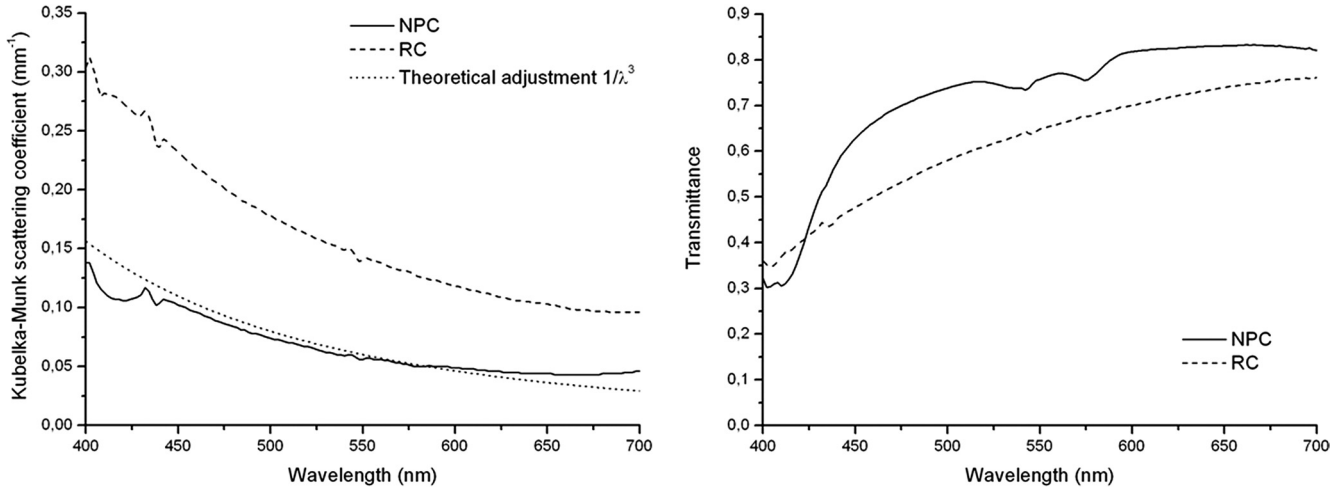

FIGURE 6. Spectral distribution of the Kubelka-Munk scattering coefficient and transmittance of the control NPCs and RCs. The theoretical adjustment demonstrating that both NPCs and RCs had a spectral dependency that was proportional to the inverse of the cube of the wavelength is shown.

scattering particles and that these particles have negligible dimensions compared with the wavelength.[34]

To determine the optical properties of the corneas, we used a simple, noninvasive method that has been widely used to evaluate the optical properties of different tissues.[35,36] By applying this method, we demonstrated that the NaCl-treated APCs showed a fiber distribution that was very similar to that of the control corneas, whereas SDS-treated APCs displayed a high level of fiber disorganization. This finding is supported by the results for the optical properties of the NaCl-treated APCs, where scattering and transmittance values were comparable to those of the control cornea.

Recellularization of acellular corneal stromas is one of the most important steps to develop a human corneal substitute in the laboratory. Although the need for repopulation of decellularized scaffolds is controversially discussed,[37] in this work we wanted to evaluate the capability of our corneal model to be repopulated by well-differentiated human keratocytes for tissue engineering purposes and to determine the optical properties of the recellularized corneas. In this context, we have described the first partial human cornea substitute that is based on decellularized porcine corneas further recellularized with human keratocytes. The method described here is able not only to maintain the structure of the native cornea, but also to offer a proper microenvironment for keratocytes to penetrate and proliferate within the stroma. Although the distribution of the cells in the native cornea could be more uniform, keratocytes were able to properly spread into the decellularized scaffold, reaching a number of cells that was very similar to that of the control corneas. In addition, the characteristic expression of ALDH1 by human keratocytes was not affected, suggesting that APCs were repopulated by mature stromal cells. ALDH1 is a distinctive marker of keratocytes that has been used in another study to distinguish differentiated keratocytes from myofibroblasts, which do not express ALDH1.[38] Moreover, this enzyme seems to act as an essential element for keeping the transparency of the cornea.[39] In the embryo, development of corneal transparency is associated with decreased light-scattering from postnatal keratocytes together with a marked increase of ALDH1 expression levels,[40] which is similar to our findings.

Our results suggest that 1.5 M NaCl treatment of porcine corneas generates an acellular corneal stroma with adequate histologic and optical properties, offering a proper microenvironment for human keratocytes to penetrate and keep their differentiation within the stroma. These substitutes recellularized with human keratocytes could have therapeutic potential. APCs with various thicknesses could be generated to repair specific defects of the corneal stroma and could eventually be used as a treatment for different kinds of corneal diseases.

References

1. Ayres BD, Rapuano CJ. Refractive power of the cornea. *Compr Ophthalmol Update.* 2006;7:243–251; discussion 253–255.
2. Li F, Carlsson D, Lohmann C, et al. Cellular and nerve regeneration within a biosynthetic extracellular matrix for corneal transplantation. *Proc Natl Acad Sci U S A.* 2003;100:15346–15351.
3. Ruberti JW, Zieske JD. Prelude to corneal tissue engineering: gaining control of collagen organization. *Prog Retin Eye Res.* 2008;27:549–577.
4. Gonzalez-Andrades M, Garzon I, Gascon MI, et al. Sequential development of intercellular junctions in bioengineered human corneas. *J Tissue Eng Regen Med.* 2009;3:442–449.
5. Kruse FE, Cursiefen C. Surgery of the cornea: corneal, limbal stem cell and amniotic membrane transplantation. *Dev Ophthalmol.* 2008;41:159–170.
6. McColgan K. Corneal transplant surgery. *J Perioper Pract.* 2009; 19:51–54.
7. Melles GR, Remeijer L, Geerards AJ, Beekhuis WH. The future of lamellar keratoplasty. *Curr Opin Ophthalmol.* 1999;10:253–259.
8. Nishida K. Tissue engineering of the cornea. *Cornea.* 2003;22: S28–S34.
9. Alaminos M, Del Carmen Sanchez-Quevedo M, Munoz-Avila JI, et al. Construction of a complete rabbit cornea substitute using a fibrin-agarose scaffold. *Invest Ophthalmol Vis Sci.* 2006;47:3311–3317.
10. Rafat M, Li F, Fagerholm P, et al. PEG-stabilized carbodiimide crosslinked collagen-chitosan hydrogels for corneal tissue engineering. *Biomaterials.* 2008;29:3960–3972.
11. Badylak SF. Xenogeneic extracellular matrix as a scaffold for tissue reconstruction. *Transpl Immunol.* 2004;12:367–377.
12. Gilbert TW, Sellaro TL, Badylak SF. Decellularization of tissues and organs. *Biomaterials.* 2006;27:3675–3683.
13. Oh JY, Kim MK, Lee HJ, Ko JH, Wee WR, Lee JH. Processing porcine cornea for biomedical applications. *Tissue Eng Part C Methods.* 2009;15:635–645.
14. Xu YG, Xu YS, Huang C, Feng Y, Li Y, Wang W. Development of a rabbit corneal equivalent using an acellular corneal matrix of a porcine substrate. *Mol Vis.* 2008;14:2180–2189.
15. Zhang C, Nie X, Hu D, et al. Survival and integration of tissue-engineered corneal stroma in a model of corneal ulcer. *Cell Tissue Res.* 2007;329:249–257.
16. Lin XC, Hui YN, Wang YS, Meng H, Zhang YJ, Jin Y. Lamellar keratoplasty with a graft of lyophilized acellular porcine corneal stroma in the rabbit. *Vet Ophthalmol.* 2008;11:61–66.
17. Wu Z, Zhou Y, Li N, et al. The use of phospholipase A(2) to prepare acellular porcine corneal stroma as a tissue engineering scaffold. *Biomaterials.* 2009;30:3513–3522.
18. Meek KM, Leonard DW, Connon CJ, Dennis S, Khan S. Transparency, swelling and scarring in the corneal stroma. *Eye.* 2003;17: 927–936.
19. Mourant JR, Canpolat M, Brocker C, et al. Light scattering from cells: the contribution of the nucleus and the effects of proliferative status. *J Biomed Opt.* 2000;5:131–137.
20. Freund DE, McCally RL, Farrell RA. Direct summation of fields for light scattering by fibrils with applications to normal corneas. *Appl Opt.* 1986;25:2739.
21. van den Berg TJ, Tan KE. Light transmittance of the human cornea from 320 to 700 nm for different ages. *Vision Res.* 1994;34:1453–1456.
22. Chinga G, Johnsen PO, Dougherty R, Berli EL, Walter J. Quantification of the 3D microstructure of SC surfaces. *J Microsc.* 2007; 227:254–265.
23. Curray J. The analysis of two-dimensional orientation data. *J Geol.* 1956;64:117–131.
24. Ragain JC Jr, Johnston WM. Accuracy of Kubelka-Munk reflectance theory applied to human dentin and enamel. *J Dent Res.* 2001;80: 449–452.
25. Lee YK. Influence of scattering/absorption characteristics on the color of resin composites. *Dent Mater.* 2007;23:124–131.
26. Thennadil SN. Relationship between the Kubelka-Munk scattering and radiative transfer coefficients. *J Opt Soc Am A Opt Image Sci Vis.* 2008;25:1480–1485.
27. Lee H, Kim M, Ko J, Lee H, Lee J, Wee W. The characteristics of porcine cornea as a xenograft. *J Korean Ophthalmol Soc.* 2006; 47:2020–2029.
28. Kampmeier J, Radt B, Birngruber R, Brinkmann R. Thermal and biomechanical parameters of porcine cornea. *Cornea.* 2000;19: 355–363.
29. Zhang C, Jin Y, Nie X, Liu Y, Lei J, Hu D. A comparative study on biocompatibility of acellular corneal stroma materials prepared by serial digestion methods (in Chinese). *Zhongguo Xiu Fu Chong Jian Wai Ke Za Zhi.* 2006;20:185–188.
30. Amano S, Shimomura N, Yokoo S, Araki-Sasaki K, Yamagami S. Decellularizing corneal stroma using N2 gas. *Mol Vis.* 2008;14: 878–882.
31. Makino H, Ota Z. Three-dimensional architecture of the mesangial matrix–comparison of the intact and acellular glomerulus. *Nippon Jinzo Gakkai Shi.* 1989;31:1039–1045.
32. Walter RJ, Matsuda T, Reyes HM, Walter JM, Hanumadass M. Characterization of acellular dermal matrices (ADMs) prepared by two different methods. *Burns.* 1998;24:104–113.

33. Bettelheim FA, Kumbar M. An interpretation of small-angle light-scattering patterns of human cornea. *Invest Ophthalmol Vis Sci.* 1977;16:233–236.
34. McCally RL, Farrell RA. *Interaction of Light and the Cornea: Absorption Versus Wavelength.* New York: Raven Press; 1988:6.
35. Hoffmann J, Lübbers DW, Heise HM. Applicability of the Kubelka-Munk theory for the evaluation of reflectance spectra demonstrated for haemoglobin-free perfused heart tissue. *Phys Med Biol.* 1998;43:3571–3587.
36. Egger HR, Blazek V. Optical properties of human brain tissue, meninges, and brain tumors in the spectral range of 200 to 900nm. *Neurosurgery.* 1987;21:459–464.
37. Lichtenberg A, Tudorache I, Cebotari S, et al. Preclinical testing of tissue-engineered heart valves re-endothelialized under simulated physiological conditions. *Circulation.* 2006;114:I559–565.
38. He J, Bazan HE. Epidermal growth factor synergism with TGF-beta1 via PI-3 kinase activity in corneal keratocyte differentiation. *Invest Ophthalmol Vis Sci.* 2008;49:2936–2945.
39. King G, Holmes R. Human ocular aldehyde dehydrogenase isozymes: distribution and properties as major soluble proteins in cornea and lens. *J Exp Zool.* 1998;282:12–17.
40. Jester JV, Lee YG, Huang J, et al. Postnatal corneal transparency, keratocyte cell cycle exit and expression of ALDH1A1. *Invest Ophthalmol Vis Sci.* 2007;48:4061–4069.